

# Investigating the Corruption Robustness of Image Classifiers with Random $L_p$ -norm Corruptions

Georg Siedel<sup>a,b,\*</sup>, Silvia Vock<sup>a</sup> and Andrey Morozov<sup>b</sup>

<sup>a</sup>Federal Institute for Occupational Safety and Health (BAuA), Germany

<sup>b</sup>University of Stuttgart, Germany

**Abstract.** Robustness is a fundamental property of machine learning classifiers to achieve safety and reliability. In the fields of adversarial robustness and formal robustness verification of image classification models, robustness is commonly defined as the stability to all input variations within an  $L_p$ -norm distance. However, robustness to random corruptions is usually improved and evaluated using variations observed in the real-world, while mathematically defined  $L_p$ -norm corruptions are rarely considered. This study investigates the use of random  $L_p$ -norm corruptions to augment the training and test data of image classifiers. We adapt an approach from the field of adversarial robustness to assess the model robustness to imperceptible random corruptions. We empirically and theoretically investigate whether robustness is transferable across different  $L_p$ -norms and derive conclusions on which  $L_p$ -norm corruptions a model should be trained and evaluated on. We find that training data augmentation with  $L_0$ -norm corruptions improves corruption robustness while maintaining accuracy compared to standard training and when applied on top of selected state-of-the-art data augmentation techniques.

## 1 Introduction

State-of-the-art computer vision models achieve human-level performance in various tasks, such as image classification [18]. This makes them potential candidates for safety-critical applications, such as in industrial environments. However, they can be easily fooled by small changes in the input data. This affects their dependability and limits trust in their ability to perform highly safety-critical tasks [3]. For classification models in particular, robustness is therefore considered a fundamental pillar of AI trustworthiness and has attracted considerable research interest in recent years.

A classifier  $g$  is locally robust at a data point  $x$  within a distance  $\epsilon > 0$ , if  $g(x) = g(x')$  holds for all perturbed points  $x'$  that satisfy

$$\text{dist}(x - x') \leq \epsilon \quad (1)$$

with  $x'$  close to  $x$  according to a predefined distance measure [3].

In the fields of adversarial attack and defence [3] as well as formal robustness verification [20], this distance measure is commonly defined mathematically by a  $L_p$ -norm distance:

$$\|x - x'\|_p = \left( \sum_{i=1}^d |x_i - x'_i|^p \right)^{1/p} \quad (2)$$

with  $d$  being the dimensionality of the data and  $p > 0$  [34, 35].

The adversarial attack domain aims at finding worst-case, lowest-distance counterexamples for robustness, while the formal robustness verification domain tries to provide a sound mathematical proof of robustness for any perturbed and possibly worst-case input.

However, the vulnerability of vision models to small changes in input data is not only true for worst-case adversarial data manipulations, but also for randomly corrupted input data [8]. Accordingly, corruption robustness aims to achieve models that perform similarly well on data corrupted with a statistical distribution. Adversarial robustness and corruption robustness<sup>1</sup> need to be clearly distinguished: Existing research suggests that training for these two robustness goals has different effects on the model behaviour and can be useful in different ways depending on the model application [30, 23]. Also, adversarial robustness and corruption robustness do not necessarily transfer to each other, and adversarial robustness is harder to achieve in high-dimensional input space [10, 12].

### 1.1 Motivation

As described above, worst-case robustness methods, such as adversarial attacks and formal robustness verification, often adapt the robustness definition based on  $L_p$ -norm distance in Equation(2). Accordingly, there exists a common set of  $L_p$ -norms, as well as a set of maximum distances  $\epsilon$  for each norm, which are applied for robustness evaluation on the most popular image classification benchmarks.  $L_\infty$ ,  $L_2$ ,  $L_1$  and  $L_0$  distances are the chosen  $L_p$ -norms [3, 20]. For the benchmark datasets CIFAR-10 or SVHN for example,  $\epsilon = 8/255$  is commonly used as the  $L_\infty$  maximum distance [35].

In contrast, in the field of corruption robustness, robustness is commonly assessed by testing artificial, but physically justifiable and empirically observed data faults originating from camera, hardware, or environment [14]. Such data faults may occur in the real world with measurable probability<sup>2</sup>. By including them in testing, such scenarios can be assured and the system can be adapted to the actual application. In this sense, such real-world corruptions are related to measuring performance under distribution shift to ensure generalization [13]. They are also relevant to risk assessment and safety, as there exists a measurable real-world probability to the risk of such corruptions.

<sup>1</sup> Also called statistical robustness

<sup>2</sup> Hence, we name them "real-world corruptions" in this paper, even though such faults are mostly artificially created in testing

\* Corresponding Author. Email: siedel.georg@baua.bund.de.

On the other hand, the definition and testing of robustness using  $L_p$ -norm distances (see Equation(2)) is much less adopted in the field of corruption robustness. We present three arguments to motivate our investigation of  $L_p$ -norm distance corruptions also in the field of corruption robustness.

First, the small amount of research on random  $L_p$ -norm corruptions shows significant negative impact on model performance even for small corruptions [30, 27]. In comparison, the adversarial robustness domain is crucially motivated by the sheer finding that image classifier performance is massively degraded on adversarial examples and in particular, that the corresponding  $L_p$ -norm corruptions sufficient for this effect are small or even imperceptible [3, 37, 22]. Even though the negative impact of random corruptions is lower compared to adversarial attacks, we propose to adapt this motivation and push corruption robustness to small or imperceptible  $L_p$ -norm distance corruptions. From our point of view, a classifier should generalize in line with human perception, regardless of whether the manipulations are worst-case or random.

Second, corruption robustness is only partially transferable across different corruption types (see Section 2). Therefore, an extensive evaluation of training and testing with random  $L_p$ -norm corruptions seems reasonable to improve the understanding of the transferability of corruption robustness.

Third,  $L_p$ -norm spheres in high dimensional input space are notoriously hard to understand in terms of what input space they cover and how they overlap. Table 1 illustrates how different the volumes of an  $L_2$ -norm sphere are from an  $L_\infty$ -norm sphere and an  $L_1$ -norm sphere as the dimensions increase.

**Table 1.** Illustration of the volume factors between  $L_\infty$ -norm sphere and  $L_2$ -norm sphere as well as  $L_2$ -norm sphere and  $L_1$ -norm sphere of the same  $\epsilon$  in  $d$ -dimensional space

$d$	$p = [\infty, 2]$	$p = [2, 1]$
3	1.9	3.1
5	19.7	6.1
10	9037	401.5
20	$6 * 10^{10}$	$4 * 10^7$

For the CIFAR-10 image dataset, which features  $32*32*3 = 3072$  dimensions, it is therefore evident why typical  $\epsilon$ -values for robustness tests differ massively between, for example,  $L_\infty$ -norm ( $\epsilon = 8/255 = 0.031$ ) and  $L_2$ -norm ( $\epsilon = 0.5$ ) [5, 4, 35]. Tests from different  $L_p$ -norm spheres can cover very different volumes and may therefore be interesting from a test coverage perspective. Comparing the overlapping volumes covered by different  $L_p$ -norm spheres can also provide insight into whether it makes sense to test on samples from various  $L_p$ -norm spheres at the same time.

## 1.2 Contributions

In this paper, we investigate the corruption robustness of image classifiers to random  $L_p$ -norm corruptions on the CIFAR-10 dataset [17]. We present results from training and test time data augmentations.<sup>3</sup> Our main contributions are as follows:

- We propose random quasi-imperceptible corruptions from different  $L_p$ -norm distances and demonstrate a significant performance

<sup>3</sup> Code available at <https://github.com/Georgsiedel/Lp-norm-corruption-robustness>

degradation when applying such corruptions at test time. We propose to compute a robustness metric based on imperceptible corruptions.

- We present evidence for an effective, previously little noticed training data augmentation strategy that improves robustness and maintains accuracy.
- We visualize and discuss the transferability of robustness across different  $L_p$ -norm corruptions. We also investigate the transferability of robustness between  $L_p$ -norm and real-world corruptions.
- We present insight into the volume overlap of different  $L_p$ -norm spheres and discuss the usefulness of testing with different  $L_p$ -norm corruptions from a test coverage perspective.

In Section 2, we summarize related work relevant to our contributions. In Section 3, we describe the sampling algorithm, robustness metrics and training setup required to perform the experiment. The results are presented and discussed in Sections 4 and 5.

## 2 Related Work

As described above,  $L_p$ -norm distances are used to define worst-case robustness. They are also used in the literature to quantify properties of image data, which in turn are used as distances for robustness evaluation. One such property is the imperceptibility threshold of image manipulations, which has been a common reference point for previous work in the field of adversarial robustness. Specifically,  $L_\infty$  manipulations of  $\epsilon = 8/255 = 0.031$  are often used in conjunction with the imperceptibility threshold [37, 22]. However, a justification of this imperceptibility threshold is loose and subjective. Researchers have therefore called for further research into "distance metrics closer to human perception" [16]. Other authors propose similarity measures for images that are more advanced than  $L_p$ -norm distances and more aligned with human perception [32, 31]. To the best of our knowledge, these measures have not yet been implemented as distance measures for robustness evaluation of perception models.

Another property of image data quantified by  $L_p$ -norm distances in the context of robustness is the average separation of classes in a dataset. This property is used by Fawzi et al. [11] in order to obtain a comparable baseline distance for robustness testing. Similarly, Yang et al. [35] measure the minimum class separation on typical image data benchmarks using  $L_\infty$ -distances, and conclude that there may theoretically exist a class separating classifier that is perfectly robust with respect to this distance. Based on this idea, some authors have proposed a reliability estimation approach in [9] and have tested on random  $L_\infty$ -corruptions with minimal class separation distance in order to obtain an interpretable robustness metric [27].

Wang et al. investigate testing and training on data corrupted by a few random  $L_\infty$  corruptions [30]. Overall, little research has been directed at evaluating robustness against various statistically distributed  $L_p$  norm corruptions.

However, it should be emphasized that several of the most common real-world corruptions used for testing and training corruption robustness in the image domain are related to  $L_p$ -norm corruptions. Gaussian noise shares similarities with  $L_2$ -norm corruptions [4]. Impulse Noise or Salt-and-Pepper Noise are similar to  $L_0$ -norm corruptions. Applying brightness or darkness to an image is a non-random  $L_\infty$  corruption that applies the same color change to every pixel.

In comparison to  $L_p$ -norm corruptions, there exists plenty of research on using real-world corruptions to evaluate corruption robustness, most notably the popular benchmark by Hendrycks et al.

[14]. Real-world corruptions and geometric transformations of images are also used for data augmentation in the training phase in order to obtain better generalizing or more robust classifiers [26]. Some training-phase augmentation approaches explicitly only target and evaluate only accuracy and not robustness [6, 24]. A few approaches use only geometric transformations, such as cuts, translations and rotations, as corruptions to improve overall robustness [36, 15]. Others use random noise types that are related to  $L_p$ -norm corruptions such as Gaussian and Impulse noise, targeting both accuracy and robustness [21, 7]. Recent efforts suggest that simple random augmentation strategies can be more effective even compared to more sophisticated augmentation strategies [24].

Although accuracy and robustness have long been considered as an inherent trade-off [29, 37], several data augmentation methods manage to increase corruption robustness along with accuracy [15, 21]. Some data augmentation methods leverage random corruptions to implicitly or explicitly improve or give guarantees for adversarial robustness [4, 33, 19, 36].

When models are trained to become more robust, the resulting robustness is typically specific to the type of corruption or attack. Only to a limited extent are adversarial or corruption robustness transferable to each other [10, 11, 25], across different  $L_p$ -norm adversarial attacks and attack strengths [2], or across real-world corruption types [14, 12].

The limited transferability of robustness motivates our investigation in transferability between  $L_p$ -norm and real-world corruptions as well as across random  $L_p$ -norm corruptions. The effectiveness of simple augmentation procedures [24] further encourages our investigation of finding such training time  $L_p$ -norm corruptions that improve corruption robustness and accuracy.

### 3 Preliminaries

#### 3.1 Sampling algorithm

In order to experiment with images with random corruptions uniformly distributed within a  $L_p$ -norm sphere, a suitable sampling algorithm that scales to high-dimensional space is required. We modify the approach of [1] to obtain a sampling algorithm that returns a corrupted image  $I_c$  for any norms  $0 < p < \infty$  with maximum distance  $\epsilon$  for a given clean image  $I$  of any dimension  $d$ :

1. Generate  $d$  random scalars  $x_i$  as components of an  $I$ -shape vector  $x$ , each drawn from a Laplace-distribution with scale parameter  $1/p$ .
2. Generate scalar  $r = w^{1/d}$  with  $w$  being a random scalar drawn from a uniform distribution of interval  $[0, 1]$ .
3. Generate  $n = (\sum_{i=1}^d |x_i|^p)^{1/p}$  to norm the sphere.
4. Return  $I_c = I + (\epsilon * r * x/n)$

$r$  is a density factor along the radius, which allows to vary the the density distribution of the data points sampled within the norm sphere. The density factor can be set to  $r = 1$  to sample with maximum corruption on the hull of the sphere instead of uniformly inside. Figure 1 visualizes 1000 samples drawn from different  $L_p$ -norms in 2D space using the proposed algorithm to demonstrate its ability to sample uniformly both inside as well as on the hull of the norm sphere.

#### 3.2 Robustness Metrics

We use three corruption robustness metrics to assess the robustness of all our trained models.

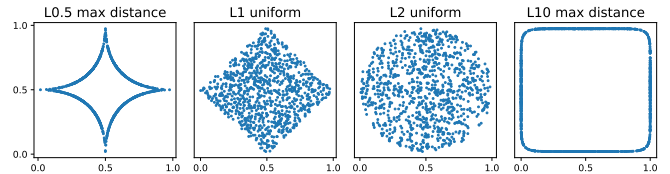


**Figure 1.** 2D samples drawn with proposed algorithm on the hull of a  $L_{0.5}$  and a  $L_{10}$  norm sphere (left and right) and uniformly from within a  $L_1$  and a  $L_2$  norm sphere (middle), all with  $\epsilon = 1$ .

**Table 2.** Sets of random  $L_p$ -norm corruptions for calculating  $mCE_{L_p}$  and  $iCE$  metrics at test time. For all  $L_0$  corruptions,  $\epsilon$  denotes the ratio of manipulated image dimensions, not the absolute number. The first three lines describe possible variants to implement  $L_0$  corruptions:  $0_{S/P}$  sets a whole pixel to 0 or 1,  $0_m$  sets one color channel to 0 or 1 and  $0_{lin}$  sets a color channel to a random value between 0 and 1.

$p$	$mCE_{L_p}$	$iCE$
	$\epsilon$	
$0_{S/P}$	[0.01, 0.02]	
$0_m$	[0.01, 0.02, 0.04]	
$0_{lin}$	[0.02, 0.03, 0.06]	
0.5	[100000, 200000, 500000]	50000
1	[40, 80, 200]	25
2	[1, 2, 4]	0.5
5	[0.2, 0.4, 1]	
10	[0.15, 0.3, 0.7]	0.06
50	[0.1, 0.2, 0.5]	0.05
200	[0.1, 0.2, 0.5]	
$\infty$	[0.02, 0.03, 0.05, 0.1]	0.01

First, we compute the  $mCE$  (mean Corruption Error) metric using the well-known corruption benchmark by [14]. As it is described as a possibility in the publication, we use a 100% error rate as a baseline. Accordingly,  $mCE$  corresponds to the average error rates  $E$  across test sets with 19 different corruptions  $c$  and 5 corruption severities  $s$  each:

$$mCE = (\sum_{s=1}^5 \sum_{c=1}^{19} E_{s,c}) / (5 * 19) \quad (3)$$

Second, we introduce a similar robustness metric  $mCE_{L_p}$ , which is calculated from the average of error rates on a set of 33  $L_p$ -norm corruptions. The different corruptions, as shown in Table 2, were empirically selected to cover different norms  $p$  and distances  $\epsilon$ .

As motivated before, achieving robustness on a set of imperceptible random corruptions can be seen as a minimal requirement for the generalization ability of a classifier. As a third metric, we propose an corresponding robustness metric, which we call  $iCE$  for "imperceptible Corruption Error", defined as

$$iCE = (\sum_{i=1}^n E_i - E_{clean}) / (n * E_{clean}) \quad (4)$$

where  $n$  is the number of different imperceptible corruptions. Since we consider performance degradation for imperceptible corruptions particularly undesirable, we choose a metric measured relative to the clean error rate  $E_{clean}$ , as found in Hendrycks et al. [14], to better illustrate relative performance degradation. Specifically for our study, we chose  $n = 6$   $L_p$ -norm distances, which are also shown in Table 2. We made the choices for selected  $L_p$  and  $\epsilon$  values based on our subjective observations of imperceptibility of corruptions on several randomly sampled maximally corrupted CIFAR-10 images. Figure 2 visualizes 3 such corruptions compared to the original image. It

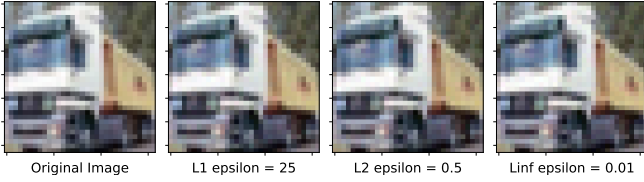


**Figure 2.** Examples from the chosen set of imperceptible corruptions

should be emphasized that this selection is highly experimental, subjective and probably not generalisable to different image datasets, dimensions or even observers. However, it is a first attempt to go beyond an arbitrary corruption severity and exploit corruptions related to human perceptual limitations. Future work should further investigate advanced distance and similarity measures more aligned with the human perception limits and develop sets of imperceptible corruptions to compute  $iCE$  for various applications.

We also report the clean error rate  $E_{clean}$ . For all reported metrics, low numbers indicate a better performance.

### 3.3 Training Setup

All experiments are performed on the CIFAR-10 classification dataset. We train a WRN-28-10 model with SGD optimizer, 0.3 dropout rate, batch size 32 and 100 epochs with a 3-step decreasing learning rate. The training data is always augmented with random horizontal flips and random crops with 4px padding. 5 runs are performed for every experiment and 95%-confidence intervals are reported to account for the stochastic nature of the training and data augmentation process.

Our goal for model training is to gain insight into whether it is beneficial to add pixel-wise  $L_p$ -norm corruptions to the potential data augmentation space with respect to the corruption robustness metrics described above. Therefore, training is performed with a broad set of  $L_p$ -norm corruptions of different  $\epsilon$  values.  $L_{0_m}$ ,  $L_{0_{in}}$ ,  $L_{0.5}$ ,  $L_1$ ,  $L_2$ ,  $L_{50}$  and  $L_\infty$  norms are used, with one separate corruption applied over the entire dataset.  $L_1(40)$  denotes a model trained exclusively on data augmented with  $L_1$  corruptions with  $\epsilon = 40$ .

In addition, we test combinations of training time corruptions by randomly combining multiple augmentations over the training process, as well as applying multiple corruptions sequentially to a single image. An overview of the corruptions used for the three models with combined corruptions can be found in Table 3. For the model denoted C1C1, 1 of 4 corruptions  $L_{0_m}$  (0.01),  $L_{0_{in}}$  (0.03),  $L_2(1)$ ,  $L_\infty(0.02)$  is randomly chosen for every training image. For C1C2, 2 of the same 4 random corruptions are randomly chosen and applied in sequence to each training image. With C2C1, we test the approach of training on a wide range of corruptions, inspired by the work of Müller et al. [24]. 1 out of 18  $L_p$ -norm corruptions<sup>4</sup> is randomly chosen for each image. Additionally, all described training procedures are compared and combined with the 3 state-of-the-art data augmentation strategies TrivialAugment (TA), RandAugment (RA) and AugMix (AM) [24, 6, 15] (see lower part of Table 4). TA+C1C2 denotes a model where the TA procedure is combined with the C1C2 augmentation sequence on each image, indicating a total of 3 sequential transformations on each training image, 1 originating from TA and 2 from the C1C2 procedure.

<sup>4</sup> The range of values can be found in the config-file on Github

**Table 3.** Sets of random  $L_p$ -norm corruptions for training the models C1C1, C1C2 and C2C1. For C2C1, the imperceptible corruptions from shown in Table 2 were used among other selected values

$p$	C1C1/C1C2	C2C1
	$\epsilon$	
$0_m$	[0.01]	[0.01, 0.02]
$0_{in}$	[0.03]	[0.02, 0.03, 0.06]
0.5		[50000, 100000]
1		[25, 40]
2	[1]	[0.5, 1]
5		[0.2]
10		[0.06, 0.15]
50		[0.05, 0.1]
$\infty$	[0.02]	[0.01, 0.02]

## 4 Results

Table 4 illustrates the performance of the described training strategies with respect to the described error metrics. From the last column, it can be observed that all models that are not trained on any  $L_p$ -norm corruptions besides  $L_0$ , are prone to imperceptible random corruptions as represented by the  $iCE$  metric.  $iCE$  values and thus a relative error rate increase of up to 10% can be observed for standard training as well as for state-of-the-art RA and TA training.

Training with individual  $L_p$ -norm corruptions, shown in the upper part of the table, improves all 3 robustness metrics  $mCE$ ,  $mCE_{L_p}$  and  $iCE$ .  $mCE_{L_p}$  is reduced more significantly than  $mCE$ , which is not surprising considering that the model is trained on such  $L_p$ -norm corruptions. For most individual corruptions, robustness is increased at the expense of an increased clean error rate. However,  $L_0$ -norm data augmentation is an exception, maintaining or slightly improving clean error rate. It also achieves even larger improvements on  $mCE$  and  $mCE_{L_p}$  values compared with other individual  $L_p$ -norm corruptions. The  $L_0$  training data augmentation therefore seems to be a promising data augmentation approach, as it is the only  $L_p$ -norm corruption that completely mitigates any trade-off between clean accuracy and robustness.

The combination of multiple corruptions through the models C1C1, C1C2 and C2C1 results in significantly improved  $mCE$  and  $mCE_{L_p}$  values. Compared with individual corruption training besides  $L_0$ -norm training, it is more effective in achieving higher robustness without sacrificing additional accuracy. Sequential application of two corruptions to single images in C1C2 shifts the trade-off between accuracy and robustness further towards the robustness side, but does not yield improvements overall. Model C2C1 achieves slightly higher accuracy and robustness than model C1C1. The accuracy of C2C1 matches the standard models accuracy while achieving far better robustness.

The lower part of Table 4 illustrates the effectiveness of the state-of-the-art data augmentation techniques RA, AM and TA. RA and TA were been evaluated with respect to corruption robustness in the original publications. We show that all three methods effectively improve both clean accuracy and robustness, with TA being the most effective technique with regards to accuracy improvement and AM with regards to robustness improvement. Our results demonstrate that TA and AM can be improved when combined with  $L_0$ -norm corruption training on top. We find this combination yields significant additional improvements in  $mCE$  and  $mCE_{L_p}$  values while maintaining or slightly improving  $E_{clean}$ . Combining TA with C1C1, C1C2 or C2C1 leads to further robustness improvements at the expense

**Table 4.** Error metrics (along columns) for various training methods (along rows). Best values in the table section are marked bold.

Model	$E_{clean}$	$mCE$	$mCE_{L_p}$	$iCE$
Standard	5.27±0.11	27.60±1.04	30.58±1.17	8.87
$L_\infty(0.02)$	5.83±0.18	23.84±1.06	20.67±1.67	-0.02
$L_\infty(0.03)$	6.43±0.30	22.58±1.14	16.81±1.00	-0.04
$L_{50}(0.1)$	5.47±0.22	23.86±1.32	21.17±1.44	0.70
$L_{50}(0.2)$	6.54±0.24	20.56±1.10	12.14±1.06	0.51
$L_2(1)$	5.68±0.13	24.94±1.34	21.77±1.36	0.36
$L_2(2)$	7.05±0.14	21.83±0.76	13.01±0.91	-0.55
$L_1(40)$	5.78±0.14	24.44±1.17	21.44±1.82	-0.19
$L_1(80)$	6.91±0.14	21.66±1.15	13.15±0.92	-0.08
$L_{0.5}(100000)$	5.82±0.16	24.03±1.06	20.11±1.43	-0.34
$L_{0.5}(200000)$	7.15±0.25	21.79±0.94	12.85±0.46	<b>-0.60</b>
$L_{0_m}(0.01)$	<b>5.19</b> ±0.15	22.52±1.67	16.55±2.33	3.37
$L_{0_m}(0.02)$	5.33±0.14	22.83±1.86	16.30±2.04	3.04
$L_{0_{in}}(0.02)$	5.23±0.15	21.59±1.00	13.27±1.13	4.01
$L_{0_{in}}(0.03)$	5.27±0.21	20.65±1.14	11.67±0.69	2.91
$L_{0_{in}}(0.06)$	5.40±0.14	19.90±1.05	9.95±0.49	1.96
C1C1	5.43±0.17	19.35±0.97	10.23±0.94	0.61
C1C2	5.59±0.09	19.26±0.68	9.63±0.40	0.60
C2C1	5.27±0.22	<b>18.56</b> ±0.94	<b>9.18</b> ±0.88	1.65
RA	4.23±0.12	18.06±1.03	18.47±1.27	8.58
AM	4.53±0.15	14.39±0.94	14.35±0.93	4.90
AM+ $L_{0_m}(0.01)$	4.54±0.15	12.64±0.75	10.18±1.27	4.14
TA	4.01±0.12	15.30±0.49	18.43±0.57	9.04
TA+ $L_{0_m}(0.01)$	<b>3.91</b> ±0.10	12.79±0.68	12.52±0.86	9.32
TA+C1C1	4.27±0.12	11.23±0.55	8.58±0.73	1.71
TA+C1C2	4.51±0.13	11.09±0.51	8.00±0.54	<b>0.49</b>
TA+C2C1	4.34±0.11	<b>10.39</b> ±0.42	<b>7.22</b> ±0.49	0.94

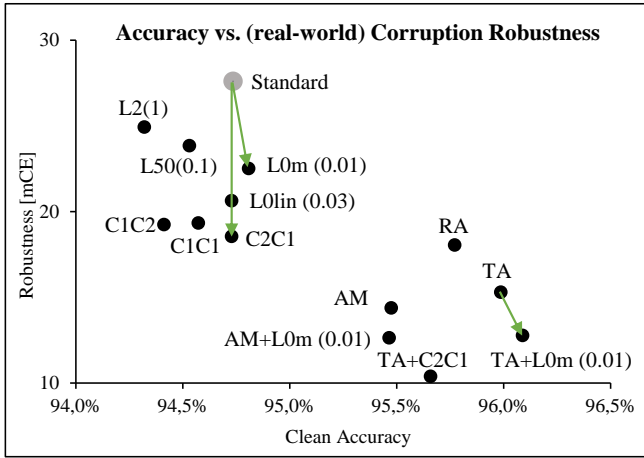


**Figure 3.** Accuracy vs. corruption robustness plot for selected models.

of clean accuracy. Not all of the described improvements meet 95% confidence intervals, but all claims are supported by the results of the best of the 5 trained models.

Figure 3 visualizes both accuracy and robustness for selected models from Table 4. Models towards the bottom right corner are both more accurate and more robust. The arrows illustrate how the models  $L_{0_m}(0.01)$ , C2C1 and TA+ $L_{0_m}(0.01)$  in particular mitigate the trade-off between accuracy and robustness compared to their baseline model without  $L_p$ -norm corruption training.

**Learning Curves** Data augmentation with training time corruptions has an implicit regularizing effect on the training process, as can be seen from the learning rate comparison in Figure 4. Compared

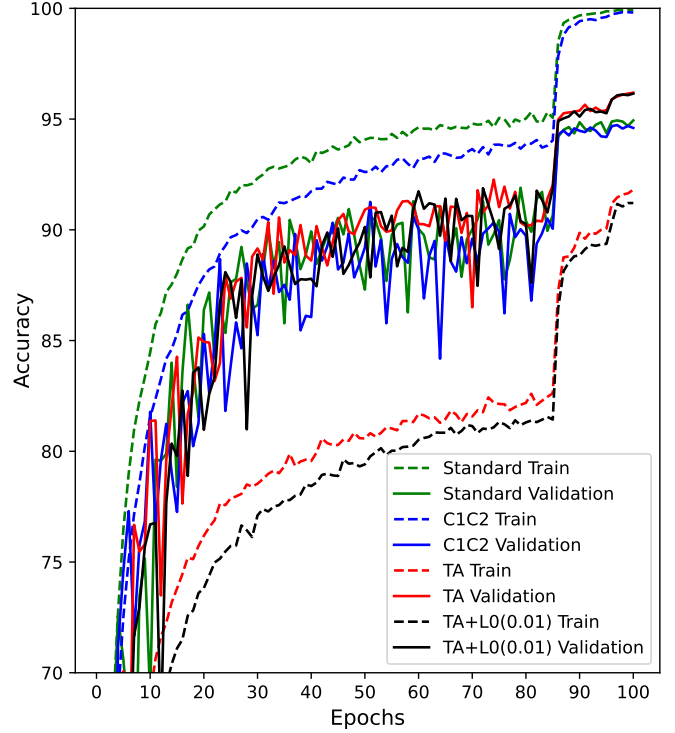


**Figure 4.** Training and validation learning curves of various models show the slight regularizing effect of  $L_p$ -norm corruption augmentation on the training process.

with standard training, the training curve is flattened with C1C2 corruptions. TA shows a strong regularization effect as the training accuracy is lower than the (clean) validation accuracy throughout the entire learning process. Additional  $L_0$ -norm corruption training further flattens the training accuracy curve of TA. The more regularized the models, the longer their training and possibly validation accuracies increase over the epochs. This may imply a positive effect of a longer training process on models trained with methods such as TA, but also with  $L_p$ -norm corruptions. Additional tests of this implication will be performed with a more adaptive learning rate schedule.

**Transferability of Robustness to Real-World Corruptions** From the full results featured in the Github repository, we derive some insight on which training data augmentations lead to robustness improvements on individual real-world corruptions represented in the  $mCE$ -metric:

- $L_p$ -norm corruption training mainly leads to improvement on pixel-wise corruptions such as Gaussian, Impulse, Speckle and Shot Noise as well as JPEG-compression and pixelation.
- $L_p$ -norm corruption training also leads to no improvements or even performance degradation on most types of blur, fog and contrast. This degradation is, on average, less significant for  $L_0$  training than for other  $L_p$  training.
- In cases where performance on individual corruptions deteriorates, increasing the corruption intensity  $\epsilon$  at training time or combining or sequencing multiple corruptions further worsens performance.
- TA, RA and AM show significant robustness improvements against all real-world corruptions.
- Combining TA, RA and AM with  $L_0$ -norm corruption training further improves robustness against pixel-wise corruptions while not significantly degrading any other real-world robustness types.



- Other additional training time corruptions such as C1C1 or C1C2 combined with TA have a degrading effect on performance against multiple real-world corruptions as described above.

**Transferability of Robustness across  $L_p$ -norms** We further visualize the individual error rates of all models trained on a single corruption on all  $L_p$ -norm corruption types. This provides insight into which  $L_p$ -norm corruption type at training time generates robustness to which  $L_p$ -norm corruption type at test time.

Figure 5 shows the normalized accuracy of models trained and tested on  $L_p$ -norm corruptions of various  $p$ . It shows that  $L_0$  corruptions at training time help the model to achieve robustness to all types of  $L_p$ -norm corruptions, slightly reduced for  $L_\infty$  corruptions. At the same time, no other training time  $L_p$ -norm corruptions except  $L_0$  itself help with effectively achieving robustness to  $L_0$ -norm corruption. Except for  $L_0$ -normal corruption, a model trained on one  $p$  does not show particularly high robustness against this or any other  $p$ .

## 5 Discussion

**Transferability of Robustness across  $L_p$ -norms** Given the limited transferability of robustness between different types of corruption known from the literature and the differences in volume factors for different  $L_p$ -norm spheres (Table 1), we expected models trained on specific  $L_p$ -norm corruptions to achieve high robustness against that type of corruption and lower robustness against less similar  $L_p$ -norm corruptions. However, we found that only training on  $L_0$ -norm corruptions transferred into good robustness against all  $L_p$ -norm corruptions. Any other attempt at  $L_p$  corruption training transferred into robustness against all  $L_p$ -norms outside  $L_0$ , no matter how similar the  $p$  between training and test corruptions.

We investigate this unintuitive behaviour by setting up an experiment to evaluate the coverage and overlap of the volumes of two different  $L_p$ -norm spheres of identical dimensionality to CIFAR-10 and certain size  $\epsilon$ . We estimate the volumes by drawing 1000 samples from inside the respective norm sphere. Figure 6 shows 6 sub-plots for 6 different  $L_p$ -norms, with their  $\epsilon$  being varied along the x-axis. The blue plots indicate how many samples from this first  $L_p$ -norm sphere are also part of a second  $L_2$ -norm sphere with  $\epsilon = 4$ . Similarly, the orange plots show how many samples from the second  $L_2$ -norm sphere are also part of the first norm sphere.

It can be seen from Figure 6, that random  $L_0$  corruptions are a special case in that their covered volume overlaps with an  $L_2$ -norm only for extreme  $\epsilon$ . There is a large interval of  $L_0 - \epsilon$ -values, where the majority of its samples are not part of the  $L_2$ -norm sphere of size  $\epsilon = 4$  and samples from this  $L_2$ -norm sphere are not part of the  $L_0$ -norm sphere either. In a slightly weaker form, this also applies to random  $L_\infty$ -norm corruptions. This implies that when comparing  $L_2$ -norms with  $L_0$ -norms or  $L_\infty$ -norms, there is a large range of  $\epsilon$ -value combinations of both norms, where the two norm spheres predominantly cover different regions of the input space. However, when comparing other  $L_p$ -norms besides of  $L_0$  and  $L_\infty$  with  $L_2$ , as has been done in the second row of Figure 6, a different result can be observed. One of the norm spheres predominantly overlaps the other in volume for the major range of  $\epsilon$ -values.

The observations from Figure 6 explain, from a coverage perspective, why corruption robustness seems to transfer between different  $L_p$ -norms outside of  $L_0$  as shown in Figure 5. However, Figure 6 does not explain why corruption robustness seems to transfer between the  $L_\infty$ -norm and other  $L_p$ -norms according to Figure 5. For

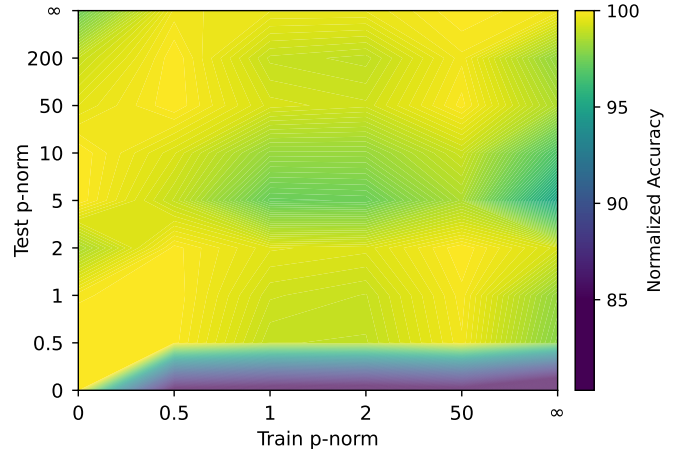


**Figure 5.** Normalized robust accuracy of models trained and tested on various  $L_p$ -norm corruptions. Accuracy of multiple epsilons is averaged for the same  $p$ . Accuracy is normalized along the "Train p-norm" axis by setting normaling the best models accuracy to 100% in order to visualize relative performance on specific test-time corruptions.

robustness testing, the  $L_\infty$ -norm corruptions seem to be a specific corner case from a coverage perspective, as its distribution differs from real-world corruptions and relatively rarely overlaps with other  $L_p$ -norm distributions. The  $L_\infty$ -norms also seem to be particularly useful in defining imperceptible corruptions for image data, since it limits the maximum color change in any single pixel. We therefore emphasize its importance even though our experiments do not show a corner-case behavior of  $L_\infty$ -norm corruptions.

Based on both Figures 5 and 6, we conclude that it may make little difference to train and test on a variety of random  $L_p$ -norm corruptions with  $0 < p < \infty$ .

This is especially true when the  $\epsilon$ -values of a set of various  $L_p$ -norm corruptions are not based on real-world observations, but are arbitrarily chosen, like the set of corruptions that the  $mCE_{L_p}$ -metric is composed of. Differences in robustness between the corruptions with  $0 < p < \infty$  are then primarily due to the relative severity of the arbitrarily chosen  $\epsilon$ -values for each  $p$ , not to differences in the type of corruption. Averaging robustness over different  $L_p$ -norm corruptions in this case is similar to simply averaging over different  $\epsilon$ -values and therefore adds little value.

**Imperceptible Corruptions** For the  $iCE$ -metric,  $\epsilon$ -values were chosen based on the motivation that various corruptions may imperceptibly small. Imperceptibility is likely to behave differently for different  $p$ , so averaging robustness over multiple  $p$  adds value to the  $iCE$ -metric. We emphasize again that this study is not suited to testing a representative, comprehensive and reliable set of corruptions that are imperceptible. Nevertheless, we find an  $iCE$ -value and therefore a relative error rate increase of nearly to 10% due to random imperceptible corruptions significant (see 4). This is especially true since  $iCE$  is equally high for the state-of-the-art data augmentation methods RA and TA. We recommend that the set of imperceptible corruptions be further developed for various computer vision applications and that a metric such as  $iCE$  be evaluated as a minimum requirement for corruption robustness.

**Promising Data Augmentation Strategies** For all models shown in Table 4,  $L_0$ -norm training data augmentation has a positive effect on robustness metrics while maintaining or improving  $E_{clean}$ . The performance degradation on some specific real-world corruptions as presented in Section 4 is less for  $L_0$ -norm training compared

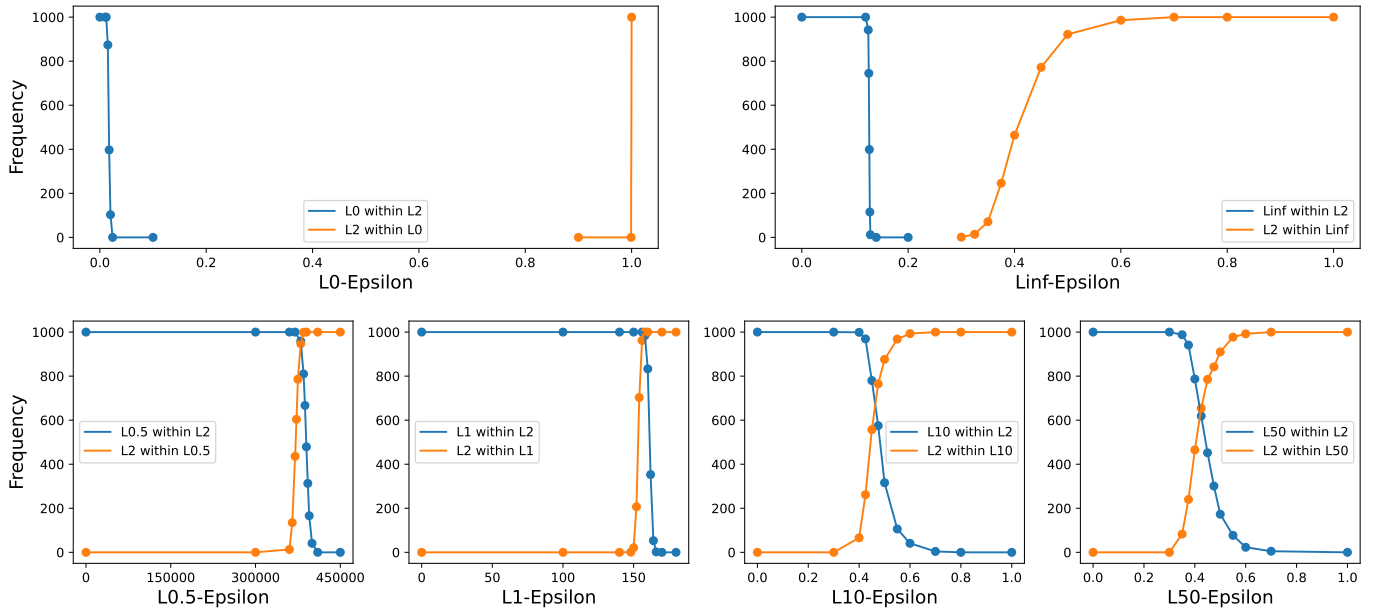


**Figure 6.** The frequency of 1000 samples drawn from inside a first CIFAR-10-dimensional  $L_p$ -norm sphere also being part of a second  $L_2$ -norm sphere of  $\epsilon = 4$  (blue plot), as well as the frequency of 1000 samples drawn from inside the second norm sphere also being part of the first norm sphere (orange plot).

with other  $L_p$ -norm training. For TA in particular, the additional  $L_0$ -norm corruption training greatly boosts the  $mCE_{L_p}$  value. This is particularly valuable since for all training strategies shown in Table 4 except TA,  $mCE_{L_p}$  is improved more than  $mCE$ . At the same time, there are no drawbacks regarding robustness to any type of real-world corruption for TA+ $L_0$  training. Overall,  $L_0$ -norm corruption training seems to be a highly recommendable augmentation strategy.

One possible explanation for the effectiveness of  $L_0$ -norm data augmentation is that it essentially represents random zeros or ones in one dimension of the input. This effect is comparable to dropout in the input layer of the network, a method that has been shown to be very effective in regularizing neural networks [28].

As tested with the C1C2 model, applying multiple corruption in sequence to individual images did not yield significant improvements. With the C2C1 model, we tested the strategy of selecting one random corruption from a particularly wide range of  $L_p$ -norm corruptions. This strategy was reported to be surprisingly effective for the TA method, using mostly real-world or geometric transformations, in [24]. C2C1 outperformed its counterpart C1C1, which features a smaller range of corruptions, in terms of corruption robustness while about maintaining accuracy. Thus, we observe the positive effect reported for TA, but the dimension of performance increase is not quite as large. The positive effect may also be solely attributable to the small  $\epsilon$  values of many of the 18 corruptions used for C2C1, see Table 3. One possible explanation that the wide range of  $L_p$ -norm training corruptions was not as effective as expected may be the limited differences of the  $L_p$ -norm spheres in volume as described above. This may limit the regularizing training effect of simply combining many of such corruptions. Nevertheless, for achieving the highest corruption robustness levels, training on a very broad range of  $L_p$ -norm corruptions in addition appears to be effective.

In the future, we plan to verify our experimental findings by conducting experiments with additional model architectures such as vision transformers, additional datasets such as Imagenet and possibly additional tasks such as object recognition or image segmentation.

## 6 Conclusion

Robustness training and evaluation with random  $L_p$ -norm corruptions is underrepresented in the literature. We trained and tested image classifiers on CIFAR-10 with random  $L_p$ -norm data augmentation. The results show that training data augmentation with  $L_0$ -norm corruptions increases robustness against real-world corruptions and  $L_p$ -norm corruptions while maintaining or slightly improving classifier accuracy. This result even holds on top of state-of-the-art data augmentation strategies. Our results indicate that robustness against  $L_0$ -norm corruptions is only effectively achieved by training on  $L_0$ -norm corruptions. In contrast, robustness against any  $L_p$ -norm corruption other than  $L_0$  can be achieved by training on any  $L_p$ -norm corruption. We discuss the reason for this result by showing that  $L_p$ -norm spheres outside  $L_0$  and  $L_\infty$  often overlap in volume. We conclude that it may not add much value to train or test on several arbitrary  $p$  outside  $L_0$  and  $L_\infty$ . Our results show that several models are negatively affected by quasi-imperceptible random corruptions. Therefore, we emphasize the need to evaluate performance on such imperceptible corruptions and propose the corresponding imperceptible corruption error metric. In the future, we plan to further investigate testing with imperceptible corruptions and training data augmentation for robustness improvement by utilizing a broader set of models and datasets.

## References

- [1] G Calafiore, F Dabbene, and R Tempo, ‘Uniform sample generation in  $l$ /sub  $p$ /balls for probabilistic robustness analysis’, in *Proceedings of the 37th IEEE Conference on Decision and Control (Cat. No. 98CH36171)*, volume 3, pp. 3335–3340. IEEE, (1998).
- [2] Nicholas Carlini, Anish Athalye, Nicolas Papernot, Wieland Brendel, Jonas Rauber, Dimitris Tsipras, Ian Goodfellow, Aleksander Madry, and Alexey Kurakin, ‘On evaluating adversarial robustness’, *arXiv preprint arXiv:1902.06705*, (2019).
- [3] Nicholas Carlini and David Wagner, ‘Towards evaluating the robustness of neural networks’, in *2017 IEEE Symposium on Security and Privacy (SP)*, pp. 39–57. Ieee, (2017).

- [4] Jeremy M. Cohen, Elan Rosenfeld, and J. Zico Kolter, ‘Certified adversarial robustness via randomized smoothing’, *International Conference on Machine Learning (ICML) 2019*, 36, (08.02.2019).
- [5] Francesco Croce and Matthias Hein, ‘Reliable evaluation of adversarial robustness with an ensemble of diverse parameter-free attacks’, in *International conference on machine learning*, pp. 2206–2216. PMLR, (2020).
- [6] Ekin D Cubuk, Barret Zoph, Jonathon Shlens, and Quoc V Le, ‘Randaugment: Practical automated data augmentation with a reduced search space’, in *Proceedings of the IEEE/CVF conference on computer vision and pattern recognition workshops*, pp. 702–703, (2020).
- [7] Wei Dai and Daniel Berleant, ‘Benchmarking robustness of deep learning classifiers using two-factor perturbation’, in *2021 IEEE International Conference on Big Data (Big Data)*, pp. 5085–5094. IEEE, (2021).
- [8] Samuel Dodge and Lina Karam, ‘A study and comparison of human and deep learning recognition performance under visual distortions’, in *2017 26th international conference on computer communication and networks (ICCCN)*, pp. 1–7. IEEE, (2017).
- [9] Yi Dong, Wei Huang, Vibhav Bharti, Victoria Cox, Alec Banks, Sen Wang, Xingyu Zhao, Sven Schewe, and Xiaowei Huang, ‘Reliability assessment and safety arguments for machine learning components in system assurance’, *ACM Transactions on Embedded Computing Systems*, (2022).
- [10] Alhussein Fawzi, Hamza Fawzi, and Omar Fawzi, ‘Adversarial vulnerability for any classifier’, *32nd Conference on Neural Information Processing Systems (NeurIPS 2018), Montréal, Canada*, (23.02.2018 2018).
- [11] Alhussein Fawzi, Omar Fawzi, and Pascal Frossard, ‘Analysis of classifiers’ robustness to adversarial perturbations’, *Machine Learning*, **107**(3), 481–508, (2018).
- [12] Nicolas Ford, Justin Gilmer, Nicholas Carlini, and Ekin Dogus Cubuk, ‘Adversarial examples are a natural consequence of test error in noise’, *Proceedings of the 36th International Conference on Machine Learning (ICML), Long Beach, California, PMLR 97, 2019*, (2019).
- [13] Dan Hendrycks, Steven Basart, Norman Mu, Saurav Kadavath, Frank Wang, Evan Dorundo, Rahul Desai, Tyler Zhu, Samyak Parajuli, Mike Guo, et al., ‘The many faces of robustness: A critical analysis of out-of-distribution generalization’, in *Proceedings of the IEEE/CVF International Conference on Computer Vision*, pp. 8340–8349, (2021).
- [14] Dan Hendrycks and Thomas Dietterich, ‘Benchmarking neural network robustness to common corruptions and perturbations’, *International Conference on Learning Representations (ICLR) 2019*, 16, (28.03.2019).
- [15] Dan Hendrycks, Norman Mu, Ekin Dogus Cubuk, Barret Zoph, Justin Gilmer, and Balaji Lakshminarayanan, ‘Augmix: A simple data processing method to improve robustness and uncertainty’, *International Conference on Learning Representations (ICLR) 2020*, 15, (05.12.2019).
- [16] Xiaowei Huang, Daniel Kroening, Wenjie Ruan, James Sharp, Youcheng Sun, Emese Thamo, Min Wu, and Xinping Yi, ‘A survey of safety and trustworthiness of deep neural networks: Verification, testing, adversarial attack and defence, and interpretability’, *Computer Science Review*, **37**, 100270, (2020).
- [17] Alex Krizhevsky, Geoffrey Hinton, et al., ‘Learning multiple layers of features from tiny images’, (2009).
- [18] Alex Krizhevsky, Ilya Sutskever, and Geoffrey E Hinton, ‘Imagenet classification with deep convolutional neural networks’, *Communications of the ACM*, **60**(6), 84–90, (2017).
- [19] Mathias Lecuyer, Vaggelis Atlidakis, Roxana Geambasu, Daniel Hsu, and Suman Jana. Certified robustness to adversarial examples with differential privacy, 2019.
- [20] Changliu Liu, Tomer Arnon, Christopher Lazarus, Christopher Strong, Clark Barrett, Mykel J Kochenderfer, et al., ‘Algorithms for verifying deep neural networks’, *Foundations and Trends® in Optimization*, **4**(3-4), 244–404, (2021).
- [21] Raphael Gontijo Lopes, Dong Yin, Ben Poole, Justin Gilmer, and Ekin D Cubuk, ‘Improving robustness without sacrificing accuracy with patch gaussian augmentation’, *arXiv preprint arXiv:1906.02611*, (2019).
- [22] Aleksander Madry, Aleksandar Makelov, Ludwig Schmidt, Dimitris Tsipras, and Adrian Vladu, ‘Towards deep learning models resistant to adversarial attacks’, *International Conference on Learning Representations (ICLR) 2018*, 28, (19.06.2017).
- [23] David Mickisch, Felix Assion, Florens Greßner, Wiebke Günther, and Mariele Motta, ‘Understanding the decision boundary of deep neural networks: An empirical study’, *arXiv preprint arXiv:2002.01810*, (2020).
- [24] Samuel G Müller and Frank Hutter, ‘Trivialaugmt: Tuning-free yet state-of-the-art data augmentation’, in *Proceedings of the IEEE/CVF international conference on computer vision*, pp. 774–782, (2021).
- [25] Evgenia Rusak, Lukas Schott, Roland S Zimmermann, Julian Bitterwolf, Oliver Bringmann, Matthias Bethge, and Wieland Brendel, ‘A simple way to make neural networks robust against diverse image corruptions’, in *Computer Vision—ECCV 2020: 16th European Conference, Glasgow, UK, August 23–28, 2020, Proceedings, Part III 16*, pp. 53–69. Springer, (2020).
- [26] Connor Shorten and Taghi M Khoshgoftaar, ‘A survey on image data augmentation for deep learning’, *Journal of big data*, **6**(1), 1–48, (2019).
- [27] Georg Siedel, Silvia Vock, Andrey Morozov, and Stefan Voß, ‘Utilizing class separation distance for the evaluation of corruption robustness of machine learning classifiers’, *The IJCAI-ECAI-22 Workshop on Artificial Intelligence Safety (AISafety 2022), July 24-25, 2022, Vienna, Austria*, (2022).
- [28] Nitish Srivastava, Geoffrey Hinton, Alex Krizhevsky, Ilya Sutskever, and Ruslan Salakhutdinov, ‘Dropout: a simple way to prevent neural networks from overfitting’, *The journal of machine learning research*, **15**(1), 1929–1958, (2014).
- [29] Dimitris Tsipras, Shibani Santurkar, Logan Engstrom, Alexander Turner, and Aleksander Madry, ‘Robustness may be at odds with accuracy’, *arXiv preprint arXiv:1805.12152*, (2018).
- [30] Benjie Wang, Stefan Webb, and Tom Rainforth, ‘Statistically robust neural network classification’, in *Uncertainty in Artificial Intelligence*, pp. 1735–1745. PMLR, (2021).
- [31] Zhou Wang, A.C. Bovik, H.R. Sheikh, and E.P. Simoncelli, ‘Image quality assessment: from error visibility to structural similarity’, *IEEE Transactions on Image Processing*, **13**(4), 600–612, (2004).
- [32] Zhou Wang and Alan C Bovik, ‘A universal image quality index’, *IEEE signal processing letters*, **9**(3), 81–84, (2002).
- [33] Tsui-Wei Weng, Pin-Yu Chen, Lam M. Nguyen, Mark S. Squillante, Akhilan Boopathy, Ivan Oseledets, and Luca Daniel, ‘Proven: Verifying robustness of neural networks with a probabilistic approach’, *Proceedings of the 36th International Conference on Machine Learning, Long Beach, California, PMLR 97, 2019*, (2019).
- [34] Tsui-Wei Weng, Huan Zhang, Pin-Yu Chen, Jinfeng Yi, Dong Su, Yupeng Gao, Cho-Jui Hsieh, and Luca Daniel, ‘Evaluating the robustness of neural networks: An extreme value theory approach’, *Sixth International Conference on Learning Representations (ICLR)*, 18, (2018).
- [35] Yao-Yuan Yang, Cyrus Rashtchian, Hongyang Zhang, Ruslan Salakhutdinov, and Kamalika Chaudhuri, ‘A closer look at accuracy vs. robustness’, *34th Conference on Neural Information Processing Systems (NeurIPS 2020), Vancouver, Canada.*, (May 2020).
- [36] Sangdoon Yun, Dongyoon Han, Seong Joon Oh, Sanghyuk Chun, Jun-suk Choe, and Youngjoon Yoo, ‘Cutmix: Regularization strategy to train strong classifiers with localizable features’, in *Proceedings of the IEEE/CVF international conference on computer vision*, pp. 6023–6032, (2019).
- [37] Hongyang Zhang, Yaodong Yu, Jiantao Jiao, Eric Xing, Laurent El Ghaoui, and Michael Jordan, ‘Theoretically principled trade-off between robustness and accuracy’, in *International conference on machine learning*, pp. 7472–7482. PMLR, (2019).